

POSTMASTECTOMY CT-BASED ELECTRON BEAM RADIOTHERAPY: DOSIMETRY, EFFICACY, AND TOXICITY IN 118 PATIENTS

MARNEE M. SPIERER, M.D.,* LINDA X. HONG, PH.D.,[†] RAQUEL T. WAGMAN, M.D.,*
MATTHEW S. KATZ, M.D.,* REBECCA L. SPIERER,[‡] AND BERYL MCCORMICK, M.D.*

Departments of *Radiation Oncology and [†]Medical Physics, Memorial Sloan-Kettering Cancer Center, New York, NY;
[‡]Edgemont High School, New York, NY

Purpose: To evaluate the technique, dosimetry, acute and late toxicity, local control (LC), and overall survival (OS) with the use of computed tomography (CT)-based postmastectomy electron beam therapy (PMEBT) in high-risk patients.

Methods and Materials: From 1990 to 2000, 118 patients with pathologic stage I-IIIb breast cancer underwent PMEBT of the chest wall (CW) ($n = 3$), CW and supraclavicular fossa (SCV) ($n = 63$), CW, SCV, and internal mammary lymph nodes (IMN) ($n = 51$), and SCV+IMN ($n = 1$). Radiation therapy was delivered with an en face electron beam with a custom cutout. Treatment plans were all CT-based. The plans of 16 patients were retrospectively reviewed to analyze dosimetry data. A retrospective chart review was conducted to assess acute and late complications, LC, and OS.

Results: At a median follow-up of 43 months, 5-year LC and OS were 91% and 61%, respectively. Sixty-one patients developed acute grade 3–4 skin toxicity, necessitating treatment breaks in 33 patients. Fifteen patients experienced a worsening of lymphedema, and 2 patients developed cardiac injury thought to be unrelated to radiotherapy. No patients developed symptomatic pneumonitis. Dosimetric analysis revealed heart and lung normal tissue complication probabilities of zero. Analysis of other clinically relevant dosimetric parameters revealed PMEBT to be comparable to previously reported techniques.

Conclusion: Postmastectomy electron beam therapy is an effective way to deliver radiation to the postmastectomy chest wall and adjacent nodal sites. It offers acceptable acute and late toxicities and a high degree of local control given the high-risk population to which it is offered. © 2004 Elsevier Inc.

Breast cancer, Postmastectomy radiotherapy, Electrons, Radiotherapy techniques.

INTRODUCTION

Recent randomized trials and a meta-analysis have demonstrated a survival advantage for high-risk patients who receive postmastectomy radiation therapy (PMRT) after adjuvant chemotherapy (1–3). However, earlier studies showed that an increase in breast cancer survival was offset by an increase in other causes of mortality, particularly cardiovascular, in those patients who underwent radiation therapy (RT) (4, 5). It is thought that the cardiac events seen in these trials were likely due to older treatment techniques and equipment. Given the potential toxicity of treatment, it is essential to use a radiation technique that optimizes chest-wall and nodal radiation while minimizing radiation dose to the heart and lungs. This is especially important with left-sided breast cancers.

Many techniques exist to treat the postmastectomy chest wall. In a recent publication, dosimetric comparisons of seven common techniques were made. No single technique was

found to deliver both the best target coverage and the lowest heart and lung complication probabilities (6). Because of the physical characteristics of electron beams, including the abrupt termination of dose and the controllable depth of penetration, since the 1950s, Memorial Sloan-Kettering Cancer Center (MSKCC) has used high-energy electrons to treat the postmastectomy chest wall. Historically, the electrons were delivered by a betatron. Treatments were well tolerated and responses were equal to that of photon irradiation (7, 8). Since 1990, conformal, computed tomography (CT)-based electron beam therapy (PMEBT) has been used to treat postmastectomy patients at MSKCC. The potential practical advantages of CT-based PMEBT are the accuracy of field design, the ability to limit radiation dose to critical normal structures, and the ease of treatment design and reproducibility of setup. In this report, we describe the technique and dosimetry, the acute and late toxicities associated with this technique, as well as disease control and survival.

Reprint requests to: Beryl McCormick, M.D., Department of Radiation Oncology, Memorial Sloan-Kettering Cancer Center, 1275 York Avenue, New York, NY 10021. Tel: (212) 639-8916;

Fax: (212) 639-2417; E-mail: spiererm@mskcc.org

Received Jan 26, 2004, and in revised form Apr 13, 2004.
Accepted for publication Apr 19, 2004.

METHODS AND MATERIALS

Patients

An Institutional Review Board–approved review of the MSKCC prospective database between 1990 and 2000 identified 118 adult female patients with pathologic Stage I–IIIB breast cancer who were candidates for PMRT and who underwent PMEBT. The decision to use PMEBT was based on clinical assessment of patients' anatomy; specifically, the degree of chest wall curvature and potential lung or heart in the radiation field. In addition, patients who had immediate breast reconstruction were not treated with PMEBT. The median age at diagnosis of breast cancer was 50 years (range, 31–78 years). Fifty percent of the patients were premenopausal. Sixty-two patients (53%) had left-sided breast cancers and 56 (47%) patients had right-sided cancers.

Surgery and pathology

A total of 116 patients underwent modified radical mastectomy (MRM) and 2 patients underwent total mastectomy (TM) after previous lumpectomy with axillary dissection. Margins were positive in 7 patients (6%), close in 9 patients (8%), negative in 62 patients (53%), and not specified in the specimens of 40 patients (34%). The median number of lymph nodes sampled was 21 (range, 1–56); the median number of positive lymph nodes was 9 (range, 0–32). Thirty-five percent of the lymph node specimens demonstrated extracapsular extension. Thirty-two patients (27%) had inflammatory breast cancer (clinically or pathologically). Pathologic staging (American Joint Committee on Cancer, 5th edition) was as follows: Stage I, 5 (4%); Stage IIA, 15 (13%); Stage IIB, 34 (29%); Stage IIIA, 22 (19%); and Stage IIIB, 41 (35%). The stage could not be determined from the records in 1 patient.

Chemotherapy and hormonal therapy

Sixty-seven patients (57%) received adjuvant chemotherapy, whereas the remainder received either neoadjuvant chemotherapy alone (7 patients) or with adjuvant chemotherapy (41 patients). Three patients did not receive any chemotherapy. Seventy patients (59%) were treated with anthracycline-based regimens. Eleven patients underwent bone marrow transplant. Seventy-three patients (62%) received adjuvant hormonal therapy.

Radiation

The chest wall (CW) alone was irradiated in 3 patients; CW and supraclavicular fossa (SCV) in 63 patients; CW, SCV, and internal mammary lymph nodes (IMN) in 51 patients; and SCV and IMN in 1 patient. The axilla was not intentionally treated; at our institution, the policy is to radiate the axilla only for undissected/inadequate dissection or gross residual disease. Beginning in 2000, the SCV was treated with photons for reasons described later in the text. These patients were not included in this review. The median dose to the initial target was 50.4 Gy (range, 42–52.2 Gy)

and the median fraction number was 28 (range, 21–29). In 88% of patients, 1.8 Gy fractions were used. The remaining patients were treated using 2.0 Gy fractions. Twenty-three percent of patients received a CW scar boost. The median boost dose was 10 Gy (range, 6–20 Gy). The median maximal target dose was 50.4 Gy (range, 42–70.4 Gy). Sixty-four percent of patients were treated with mixed energy electron beams.

Simulation

The patients were immobilized in the supine position using customized cradles (Alpha Cradle Molds, Akron, OH) with the ipsilateral arm raised above the head and the contralateral arm by the side. Attempts were made to have the ipsilateral arm lay as flat as possible. This was done to ensure that a 25×25 electron cone could be as close to the patient as possible without hitting the arm. After the patient was positioned, the physician marked the outline of the CW and SCV fields, and wires were placed over the marks and the mastectomy scar. The medial and lateral borders of the CW field were determined by the mastectomy incision; specifically, 1–2 cm beyond the incision. The inferior border was 2 cm below the contralateral inframammary fold, and the superior border was the clavicle (junction of the SCV field). The superior border of the SCV field was 2 cm above the first rib. The medial and lateral borders were the pedicles of the spine and humeral head, respectively. A separate wire was occasionally placed on the junction of the CW and SCV fields as indicated by the physician. A radiopaque marker was also placed over the SCV field prescription point, as indicated by the physician. For patients who needed the IMN treated, a separate wire was placed to outline the IMN field. For some patients, the CW/IMN/SCV fields were simulated with a single isocenter with a 25×25 electron cone encompassing all the wires. For those patients whose wires extended outside a single 25×25 cone, two isocenters were created: one for the CW/IMN field and the other for the SCV field. The CW/IMN isocenter was set by centering the $25 \text{ cm} \times 25 \text{ cm}$ collimator in the lateral and cephalad-caudad directions within the area defined by the CW/IMN wires. The SCV isocenter was determined by shifting the table superiorly only from the CW/IMN isocenter to the CW and SCV junction. The two isocenters were then tattooed on the patient, along with alignment and junction points. [Figure 1](#) shows a three-dimensional view of a patient with the central axis tattoo and alignment tattoos. Before CT simulation was available (April 1998), all patients were simulated conventionally and then a treatment planning CT scan was obtained. All patients treated since April 1998 were simulated on a CT simulator (Phillips-Marconi PQ 5000 AcQsim, Picker International, Highland Heights, OH).

Treatment planning

For the CW/IMN electron field, the gantry angle was chosen so that the beam direction was approximately perpendicular to the skin surface and optimal over the entire

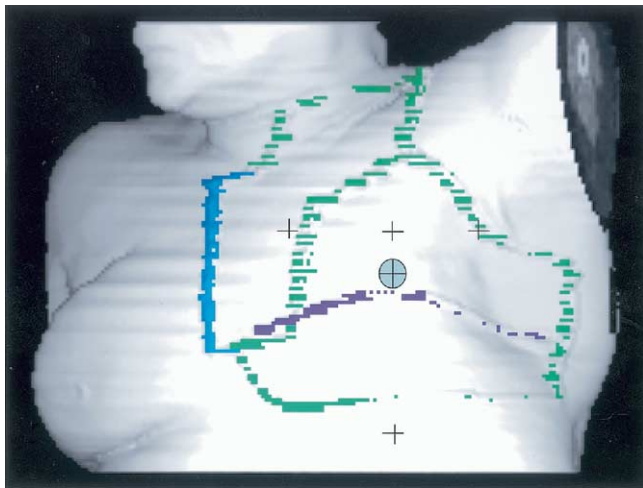


Fig. 1. Three-dimensional view of patient. Purple = scar wire; blue = IMN wire; \oplus = central axis tattoo for CW field; + = alignment tattoo.

CW/IMN region. Treatment source to skin distance (SSD) was normally set at 105 cm, even though up to 110 cm SSD was used for some patients because of clearance issues. An aperture for the CW/IMN field was created by outlining the CW/IMN field wire and the CW/SCV junction on the patient's skin surface. A single base flap of tissue-equivalent bolus was placed over the entire CW/IMN field to bring full dose to the skin. The electron beam energy was selected to be the lowest electron energy that would allow the depth of the exiting 90% isodose level to be at least as deep as the thickest part of CW, including the thickness of the bolus. The thickness of the base flap bolus was determined to be the entrance depth of the 90% isodose level of the electron beam to ensure that the skin would receive full dose for a prescription level of 90%. Mixed energy electron beams were used in 64% of the patients, 12 MeV in 20%, 9 MeV in 15%, and 15 MeV in 1 patient. Because of CW thickness variation, small pieces of additional bolus were added so that the prescription isodose line (90%) would follow the CW interface throughout the entire CW region. Dose distributions were evaluated on transverse slices every 2 cm throughout the fields. Custom bolus layers were interpolated between slices. Because of the obliqueness of the peripheral contour of the patient, a boost field with the same gantry angle as the main CW field was often added to improve coverage. This had a peripheral medial, lateral, or superior aperture, and the energy was typically the same as or higher than the main CW field. This boost field typically accounted for 10% of the prescription dose, with a range of 8–20%. For those patients whose IMNs were treated, a peripheral medial boost field with the same or higher electron energy was often needed.

For the SCV electron field, the beam direction was set to be anteroposterior for the majority of patients. Treatment SSD was normally set at 105 cm, even though as much as 110 cm SSD was used for some patients, again because of clearance issues. An aperture for the SCV field was created

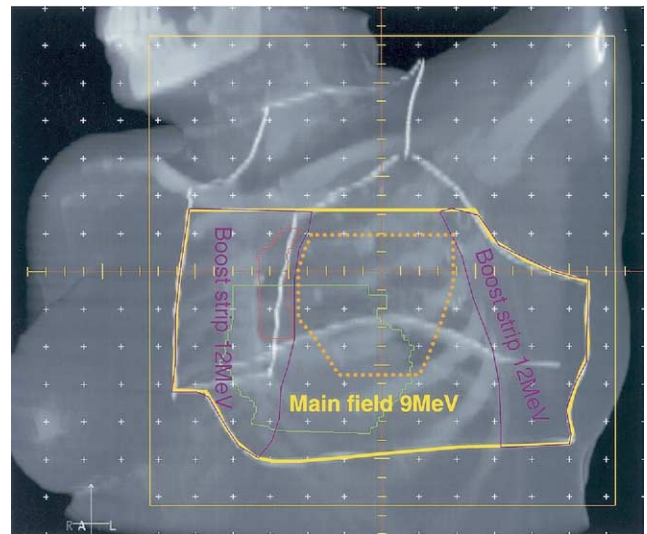


Fig. 2. Digital composite radiograph of chest wall field. Contours: red = internal mammary nodes (IMN); green = heart; orange = custom bolus

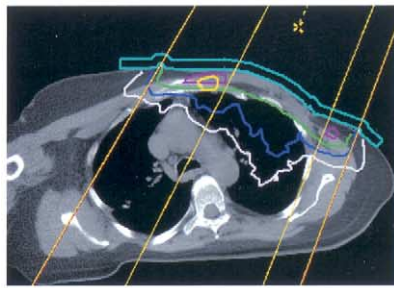
by outlining the SCV wire and the CW/SCV junction on the patient skin surface. No bolus was used for the SCV field. The electron beam energy for the SCV field was chosen so that the depth of the exiting 90% isodose level would be adequate for the supraclavicular nodes. To improve the dosimetric match between the CW/IMN and the SCV field, the junction was shifted by 1 cm daily. Therefore, on an every-other-day basis, the CW/IMN electron field apertures were reduced by 1 cm superiorly and the SCV field aperture was increased by 1 cm inferiorly.

Customized bolus was constructed according to the beam's eye-view projection from the treatment planning system and then attached to the base flap bolus with alignment markers relative to the CW/IMN isocenter. The whole bolus assembly was then placed on the patient reliably on a daily basis. Figure 2 illustrates a digital composite radiograph (DCR) of a CW plan; Fig. 3 illustrates the isodose distribution for the CW treatment plan.

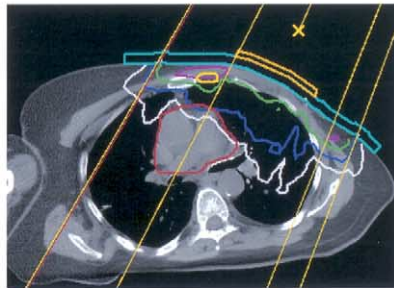
Treatment verification and daily setup

On setup day, the physician and physicist visually inspected the fields, including the moving junctions, on the patient. Portal films were taken using photon beams for the purpose of documentation.

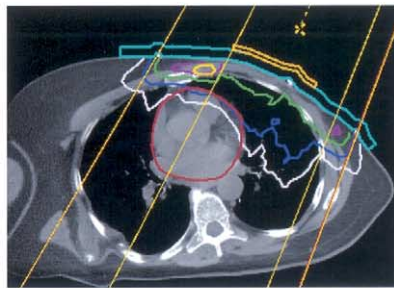
For the CW/IMN field, the therapists did the following: (1) setup SSD to the specified distance on the CW tattoo, (2) rotated the gantry to the specified angle, (3) shifted the table laterally only back to the CW tattoo, (4) inserted the CW aperture, and (5) marked the superior CW field border. For the SCV photon field, the therapists did the following: (1) shifted the table longitudinally to the SCV tattoo, (2) setup SSD to the specified distance, (3) rotated the gantry to the specified angle, and (4) shifted the table longitudinally if necessary to match the marked CW superior border.



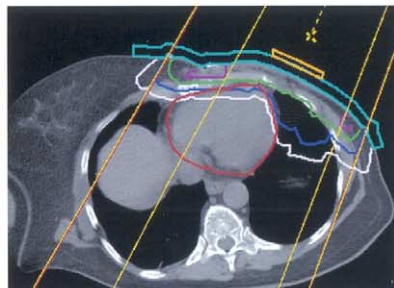
(a) superior 2 cm plane



(b) central axis plane



(c) inferior 2 cm plane



(d) inferior 6 cm plane

Fig. 3. Isodose distribution for a chest wall treatment plan. Isodose level: magenta = 105%; green = 90% (Rx); blue = 50%; white = 10%. Contours: yellow = internal mammary nodes (IMN); red = heart; cyan = 1 cm base bolus; yellow = 5 mm custom bolus.

Dosimetric analysis

Dosimetry data were obtained retrospectively for this study. The simulation CT scans and treatment plans of all patients scanned after 1997, when archiving was initiated, were used as representatives of the study group. Of the 18 patients simulated during this time, the scans of 2 could not be retrieved. Thus, the dosimetry data are based on the 16 patients (8 patients who were treated to their CW and SCV and 8 patients who were treated to their CW, SCV, and IMNs; 12 patients had left-sided tumors) whose scans were

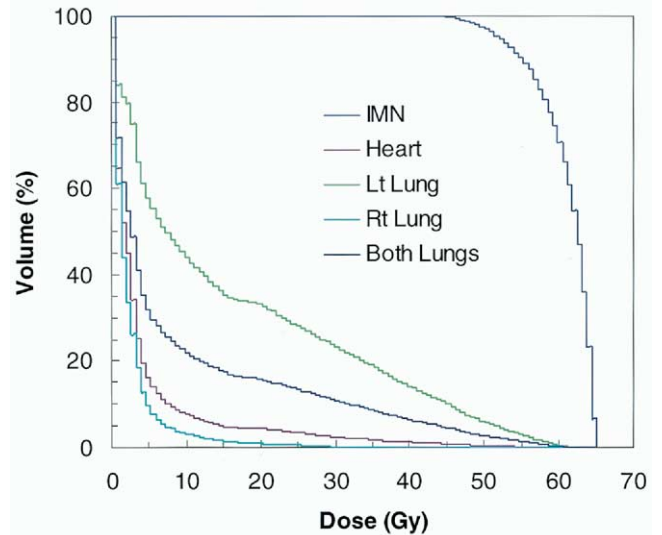


Fig. 4. Dose–volume histogram for a left-sided chest wall patient with internal mammary lymph nodes treated. Rx = 50.4 Gy.

archived and evaluable. The internal mammary lymph nodes were contoured in the fashion described by Pierce *et al.*; only those located in interspaces one to three were included (6). The heart was contoured in two ways: (1) every CT slice that contained pericardium was included and (2) the entire heart excluding the great vessels as described by Pierce *et al.* was included. The former was done to best approximate the risk of pericardial toxicity and the latter was done to assess the risk of ischemic heart disease and to compare the results with those obtained by Pierce *et al.* The patients' external surface and lung contours were done by automated density tracking and then edited. One physicist (L.H.) reviewed the treatment plans of each patient and calculated all the dose–volume histograms (DVH). DVHs were calculated for the IMNs, heart, ipsilateral lung, and bilateral lungs as shown in Fig. 4. The IMN median dose, volume of heart that received >30 Gy (median V30), volume of ipsilateral and total lung that received >20 Gy (median V20), dose that 5% of the heart and ipsilateral lung received (median D05; by convention, a measure of hot spots), and the normal tissue complication probability (median NTCP) of the heart and lungs were calculated. Only the 12 left-sided tumors were included in the calculations for the heart V30, D05, and NTCP. These parameters were chosen to compare the results with those reported by Pierce *et al.*

Follow-up and statistical analysis

The median follow-up time, calculated from the date radiation was completed, was 43 months (range, 1–143 months). Patients were followed according to National Comprehensive Cancer Network (NCCN) Clinical Practice Guidelines (history and physical examination every 4–6 months for 5 years, then every 12 months) (9), often alternating between their medical, radiation, or surgical oncol-

ogist. Data on acute and late toxicities were based on the Radiation Therapy Oncology Group (RTOG) grading scale. Local recurrence was defined as tumor recurrence in the irradiated portal. Data on overall survival are irrespective of cause. Actuarial rates were calculated with the Kaplan-Meier product-limit method (10).

RESULTS

Dosimetry

For the patients included in the dosimetric analysis, the IMN median dose was 53 Gy (range, 50–60 Gy). The median heart V30 was 6.80% (range, 1.29–22.98%). The median ipsilateral lung V20 was 38.03% (range, 21.68–59.55%), and the median total lung V20 was 20.39% (range, 9.06–29.77%). The median heart D05 was 34 Gy (range, 0.8–53 Gy), and the median lung D05 was 51 Gy (range, 46–55 Gy). Both the heart and lung NTCPs were zero.

Clinical toxicity

Of the 118 patients treated, 36 patients (31%) required treatment breaks lasting a median of 7.5 days (range, 1–20 days). In 33 patients (28%), this was due to acute toxicity of treatment. Sixty-one patients (52%) developed acute RTOG Grades 3–4 skin toxicity (60 patients, Grade 3; 1 patient, Grade 4). All other acute toxicities (fatigue, edema, pruritus, and rash) were Grade 2 or less. One patient developed late Grade 4 skin toxicity.

Lymphedema of the ipsilateral arm developed in 30 patients (25%). Half of these patients noted their edema had been unchanged since the postoperative period, before the initiation of RT.

Two patients developed cardiac injury; both patients had left-sided cancers. One patient did not have any history of cardiovascular disease at diagnosis of breast cancer. Postoperatively, she was treated with eight cycles of cyclophosphamide, methotrexate, and fluorouracil chemotherapy. She was then treated with 50.4 Gy in 28 fractions to the CW and SCV regions using mixed electron energies and custom bolus. She developed metastatic disease 1 year and 3 months after completing RT and was treated with several (nonanthracycline) chemotherapies. She developed a local recurrence 3 years and 8 months after completing RT, and at this time was treated with doxorubicin. She had a normal multiple gated acquisition scan before beginning therapy. She developed dyspnea 3 months after initiating therapy, and an echocardiogram done 8 months after initiating therapy revealed global left ventricular dysfunction, supporting the diagnosis of congestive heart failure. This was thought to be due to anthracycline-induced cardiomyopathy. The second patient had a history of hypertension. Postoperatively, she was treated with four cycles of doxorubicin, cyclophosphamide, and paclitaxel chemotherapy. She was then treated with 50.4 Gy in 28 fractions to the CW and SCV regions using mixed electron energies and custom bolus. She developed dyspnea 3 years and 7 months after completing treatment with doxorubicin (3 years and 4

months after completing RT). An echocardiogram revealed an ejection fraction of 20% supporting the diagnosis of congestive heart failure. This was thought to be due to many years of uncontrolled hypertension. The contribution of radiation to both patients' cardiac disease is unknown; however, the treating physicians felt that it was unlikely to be a clinically significant factor.

Six patients developed subsequent malignancies (1 acute myelogenous leukemia; 1 contralateral breast; 1 pancreas; 2 uterus; 1 kidney). All were thought unrelated to PMEBT.

No rib fractures, brachial plexopathies, or symptomatic pneumonitis were reported.

Local control and survival

The 5-year actuarial local control (LC) was 91%. Seventy-one patients (60%) were alive at the time of analysis. Of the 47 who died, 40 died from breast cancer, 3 from other malignancies, and 1 from complications of diabetes. Three died of unknown causes. The 5-year actuarial overall survival was 61%. At last follow-up, 53% of patients are without evidence of disease.

DISCUSSION

For patients who require RT after mastectomy without reconstruction for locally advanced breast cancer, CT-based electron beam therapy has been used as adjuvant treatment at MSKCC since 1990. Merits of PMEBT using CT planning include individualized, conformal treatment, relative ease and reproducibility of setup, acceptable acute toxicity, minimal long-term toxicity, and a high degree of local control and overall survival given the high-risk population.

Use of electrons has recently been reported in this population; however, CT planning was performed only on a minority of patients in these series (11). Because of variation of patients' CW thickness, we believe that CT-based planning is necessary for accurate electron beam energy selection and bolus design to ensure optimal target coverage while minimizing normal tissue dose.

Treatment with electrons has also been described using the electron arc technique. This technique requires mechanical modifications of the linear accelerator and additional dosimetric studies of the collimator systems. With electron arc treatment, it is also necessary to use tertiary collimation placed on or near the patient's thorax to sharply define the treatment volume and to shield normal tissue outside the treatment volume (12, 13). In contrast, one of the main advantages of CT-based electron beam treatment is ease of setup. For this technique, the therapists follow a few well-defined steps; subsequently, the possibility for error is small and setup time and treatment time together take a total of 15 min. In addition, for IMN patients, cold or hot spots are avoided because of matching of the CW field with the IMN field; they are treated within one gantry angle.

To evaluate our dosimetry and the predicted risk of late toxicity with this technique, we retrospectively reviewed the plans of 16 patients whose scans had been archived and

were evaluable. For comparison, we used the data reported by Pierce *et al.* as a guideline. However, several factors limit a direct comparison, including dose consistency and target volume delineation. In the dosimetric article by Pierce *et al.*, all the relevant planning parameters were kept constant; the prescription dose for all 20 “virtual” patients was 50 Gy in 2 Gy fractions and the CW planning target volume was delineated on the axial CT scans by the rib–soft tissue interface posteriorly, 1 cm lateral to the midline catheter medially, 1 cm medial to the midaxillary catheter laterally, and 1 cm inside the superior and inferior catheters (6). In our study, the median dose for the 16 patients used in dosimetric analysis was 50.4 Gy (range, 42–50 Gy) using 1.8 Gy fractions in 88% of the cases. Of note, in these patients, we have excellent target coverage; our CW received the full prescription dose, whereas our IMNs received more than prescription. Although our median dose was the same as that described by Pierce *et al.*, our CW planning target volume was often quite different. In the majority of our patients, to cover the entire mastectomy incision, the medial and lateral borders often extended past midline medially and well past the midaxillary line laterally.

Perhaps the greatest concern with PMRT is its association with cardiac toxicity. Since the late 1960s, the term radiation-induced heart disease (RIHD) has been used with regard to the clinical and pathologic conditions resulting from injury to the heart during therapeutic radiation. Pericardial, myocardial, and accelerated coronary artery disease are all possible delayed RIHD syndromes. Cardiac toxicity can be seen months to years after irradiation (5, 14–23). Data have shown that the favorable effect of radiation therapy on mortality from breast cancer was offset by an increase in nonbreast cancer deaths, specifically vascular. It is speculated that the cardiac events seen in these trials were likely the result of older treatment techniques and equipment (4, 5, 15). However, even with the use of contemporary megavoltage treatment for left-sided tumors, the left anterior descending coronary artery receives substantial doses of radiation (16, 17). In the analysis of patients treated in the Danish Trials 82b and 82c, those who were treated with anterior electron beams to the chest wall and internal mammary nodes did not demonstrate the increased risk of RIHD at a median follow-up time of 10 years (18, 19). Similarly, in the Stockholm trial, only patients who received the highest doses of radiation (treated with tangential Co60 fields for left-sided tumors) were found to have a significantly increased risk of death resulting from ischemic heart disease compared with surgical controls. No increased risk was observed in patients with right-sided tumors or with patients treated with electrons (15). Furthermore, the influence of chemotherapy is very important; doxorubicin is a well-known cardiotoxin whose principal effects are on the myocardium. Patients who receive doxorubicin and RT to their hearts are at an increased risk of developing cardiac damage (20, 21). In our series, 59% of the patients in this series were treated with anthracycline-based regimens. Only 2 patients suffered clinically identifiable cardiac injury; 1 was thought

to be due to doxorubicin and the other to long-standing hypertension.

In terms of our heart dose, the median V30 was 6.80% and our NTCP was zero. Our V30 is similar to the electron plan described by Pierce *et al.* and slightly higher than the other techniques, whereas our NTCP is the lowest of all the methods. Our relatively high V30 may be explained by the fact that, in contrast to Pierce *et al.*, we contoured every slice that included pericardium to best approximate the risk of pericardial toxicity as well as ischemic heart disease. However, even when we contoured in the fashion described by Pierce *et al.* (whole heart excluding great vessels), the median V30 was only slightly lower than the median V30 calculated with every slice that included pericardium. The incongruity between the NTCP and the V30 can be explained by the shape of our DVH (see Fig. 4). Although 6.8% of the heart received a low dose, very little of the heart received a high dose; the median heart D05 was only 34 Gy. V30 was chosen as an important parameter based on the work of Gagliardi *et al.*, whose data suggested that a dose of 30 Gy or more correlated to an increased risk of RIHD (22). Importantly though, data from Ericksson *et al.* in an analysis of Hodgkin’s patients found that not only was the V30 important, but also that the risk of RIHD increased as the volume irradiated to higher doses increased (23). Therefore, although a larger area of the heart received RT, a much smaller area got what is likely to be a clinically significant dose; this explains our low NTCP. Longer follow-up and prospective assessment of cardiac function are needed to fully quantify long-term cardiac morbidity. Improvements in imaging techniques may also help to better identify the impact of radiation therapy on both the small and large vessels of the heart.

Radiation pneumonitis is a well-defined clinical syndrome associated with lung irradiation that typically develops up to 6 months after completion of therapy. One contributing risk factor to the development of pneumonitis is the volume of lung irradiated (24, 25). The median ipsilateral lung V20 in our series was 38.03% and median total lung V20 was 20.39%. The NTCP was zero. The total lung V20 was chosen as an important parameter based on the work of Graham *et al.*, which showed it to be a significant predictor of Grade 2 or greater pneumonitis. In that series, a V20 of <22 carried with it a 0% risk of Grade 2 or greater pneumonitis. The authors stated in their discussion that in clinical practice, as long as the V20 is <25%, dose escalation is possible due to the very low risk of pneumonitis (25). In our series, we did not have any patients who had symptomatic pneumonitis, which corroborates the data by Graham *et al.* Our relatively high ipsilateral lung V20 but low NTCP may be explained by two factors. First, and most important, the shape of our DVH is characteristic of electron beam therapy. Although at low doses (V20), a relatively large volume of lung is irradiated, at higher doses, very little of the lung is irradiated. Second, our CW target area, as defined medial-to-lateral by the mastectomy incision plus 1–2 cm, was typically larger than that described by Pierce *et*

al. It was common for our medial border to extend to the contralateral CW and for our lateral border to be posterior to the midaxillary line. It is probable that these larger target volumes resulted in a larger volume of lung being irradiated.

The predominant acute toxicity in our series was skin-related. Fifty-two percent of the patients in our series developed RTOG Grades 3 and 4 skin toxicity; 28% required treatment breaks because of this toxicity. This is higher than expected with tangents; however, the clinical implications of these treatment breaks are unknown; although 28% required breaks, our LC was excellent. Many previous reports on PMRT do not report on acute skin toxicity (1, 2, 11, 26). Moist desquamation occurred in 22% of the patients using the electron arc technique (11). Data concerning toxicity necessitating treatment breaks were not reported in any of the series. Much of the skin toxicity developed in the SCV field because of the contour of the clavicle and the resultant electron scatter. For the past 3 years, we have treated the SCV with photons (with the gantry angle 10° off anteroposterior to be off cord) and our skin toxicity in this area has been markedly reduced. In our series, all other acute toxicities (fatigue, edema, pruritus, and rash) were Grade 2 or less and are to be expected.

Upper extremity lymphedema is a well-known complication of axillary lymph node dissection. In the surgical literature, the incidence ranges from 1% to 38% depending on whether or not a full dissection was completed (27). The axilla was not intentionally treated in this group of patients, despite the fact that 35% had extranodal extension. At our

institution, the policy is to radiate the axilla only for undissected/inadequate dissection or gross residual disease. This is based on data that suggest extranodal extension is a predictor for distant disease rather than local failure (28, 29). With an adequate axillary lymph node dissection, the rate of local failure is low, whereas morbidity is high. Despite this, lymphedema was the predominant late toxicity occurring in 25% of our patients. However, half of these patients reported having the same degree of lymphedema before initiating radiation. Other series report incidences of 10–46% after axillary lymph node dissection and radiation therapy (12, 18, 30).

The 5-year actuarial local control and survival rates were 91% and 61%, respectively. These are comparable to other techniques (1, 2, 11, 12), given that 83% of our patients were Stage IIB or higher.

CONCLUSION

CT-based electron beam therapy is an effective way to deliver RT to the postmastectomy chest wall. In selected patients, it significantly decreases the volume of normal tissue receiving high doses of radiation. To date, it appears to offer acceptable acute and late toxicities and a high degree of local control and survival given the high-risk population to which it is offered. Further study is needed to define both the long-term impact of this technique and the impact of increasing use of anthracycline-based chemotherapy in conjunction with radiation therapy on long-term cardiac morbidity and mortality.

REFERENCES

- Overgaard M, Hansen PS, Overgaard J, *et al*. Postoperative radiotherapy in high-risk premenopausal women with breast cancer who receive adjuvant chemotherapy. *N Engl J Med* 1997;337:949–955.
- Ragaz J, Stewart MJ, Le N, *et al*. Adjuvant radiotherapy and chemotherapy in node-positive premenopausal women with breast cancer. *N Engl J Med* 1997;337:956–962.
- Whelan TJ, Julian J, Wright J, *et al*. Does locoregional radiation therapy improve survival in breast cancer? A meta-analysis. *J Clin Oncol* 2000;18:1220–1229.
- Early Breast Cancer Trialists' Collaborative Group. Favourable and unfavourable effects on long-term survival of radiotherapy for early breast cancer: An overview of the randomized trials. *Lancet* 2000;355:1757–1770.
- Cuzick H, Stewart L, Rutqvist J, *et al*. Cause-specific mortality in long-term survivors of breast cancer who participated in trials of radiotherapy. *J Clin Oncol* 1994;12:447–453.
- Pierce LJ, Butler JB, Martel MK, *et al*. Postmastectomy radiotherapy of the chest wall: Dosimetric comparison of common techniques. *Int J Radiat Biol Phys* 2002;52:1220–1230.
- Chu FH, Scheer AC, Gaspar-Landero J. Electron-beam therapy in the management of carcinoma of the breast. *Radiology* 1960;75:559–567.
- Chu FH, Nisce L, Laughlin JS. Treatment of breast cancer with high-energy electrons produced by 24-mev betatron. *Radiology* 1963;81:871–880.
- Carlson RW, Anderson BO, Edge SB, *et al*. NCCN Breast Cancer Practice Guidelines Panel: NCCN. *Breast Cancer* 2003;1:148–188.
- Kaplan EL, Meier P. Non parametric estimation from incomplete observations. *J Am Stat Assoc* 1958;53:457–481.
- Feigenberg SJ, Mendenhall NP, Benda RK, *et al*. Postmastectomy radiotherapy: Patterns of recurrence and long-term disease control using electrons. *Int J Radiat Oncol Biol Phys* 2003;56:716–725.
- Gaffney DK, Leavitt DD, Tsodikov A, *et al*. Electron arc irradiation of the postmastectomy chest wall with CT treatment planning: 20-year experience. *Int J Radiat Oncol Biol Phys* 2001;51:994–1001.
- Hehr T, Budach W, Paulsen F, *et al*. Evaluation of predictive factors for local tumor control after electron beam-rotation irradiation of the chest wall in locally advanced breast cancer. *Radiother Oncol* 1999;50:283–289.
- Stewart JR, Fajardo LF, Gillette SM. Radiation injury to the heart. *Int J Radiat Oncol Biol Phys* 1995;31:1205–1211.
- Rutqvist LE, Lax I, Fornander T, *et al*. Cardiovascular mortality in a randomized trial of adjuvant radiation therapy versus surgery alone in primary breast cancer. *Int J Radiat Oncol Biol Phys* 1992;22:887–896.
- Fuller SA, Haybittle JL, Smith RE, *et al*. Cardiac doses in post-operative breast irradiation. *Radiother Oncol* 1992;25:19–24.
- Janjan NA, Gillin MT, Prows J, *et al*. Dose to the cardiac vascular and conduction systems in primary breast irradiation. *Med Dosim* 1989;14:81–87.
- Hojris I, Overgaard M, Christensen JJ, *et al*. Morbidity and mortality of ischemic heart disease in high-risk breast cancer patients after adjuvant postmastectomy systemic treatment

- with or without radiotherapy: Analysis of DBCG 82b and 82c randomized trials. Radiotherapy Committee of the Danish Breast Cancer Cooperative Group. *Lancet* 1999;354:1425–1430.
19. Hojris I, Andersen J, Overgaard M, *et al.* Late treatment-related morbidity in breast cancer: Patients randomized to postmastectomy radiotherapy and systemic treatment versus systemic treatment alone. *Acta Oncologica* 2000;39:355–372.
 20. Von Hoff DD, Layard MW, Basa P, *et al.* Risk failures for doxorubicin-induced congestive heart failure. *Ann Intern Med* 1977;91:710–711.
 21. Billingham ME, Briston MR, Glatstein E, *et al.* Adriamycin cardiotoxicity: Endomyocardial biopsy evidence of enhancement by irradiation. *Am J Surg Pathol* 1977;1:17–23.
 22. Gagliardi G, Lax I, Soderstrom S, *et al.* Prediction of excess risk of long-term cardiac mortality after radiotherapy of stage I breast cancer. *Radiother Oncol* 1998;46:63–71.
 23. Ericksson F, Gagliardi G, Liedberg A, *et al.* Long-term cardiac mortality following radiation therapy for Hodgkin's disease: Analysis with the relative seriality model. *Radiother Oncol* 2000;55:153–162.
 24. Kimsey FC, Mendenhall NP, Ewald LM, *et al.* Is radiation treatment volume a predictor for acute or late effect on pulmonary function? A prospective study of patients treated with breast-conserving surgery and postoperative radiation. *Cancer* 1994;73:2549–2555.
 25. Graham MV, Purdy JA, Emami B, *et al.* Clinical dose-volume histogram analysis for pneumonitis after 3D treatment for non-small cell lung cancer (NSCLC). *Int J Radiat Oncol Biol Phys* 1999;45:323–329.
 26. Hardenbergh PH, Bentel GC, Prosnitz LR, *et al.* Postmastectomy radiotherapy: Toxicities and techniques to reduce them. *Semin Radiat Oncol* 1999;9:259–268.
 27. Kissin MW, Querci della Roveret G, Easton D, *et al.* Risk of lymphoedema following the treatment of breast cancer. *Br J Surg* 1986;73:580–584.
 28. Hetelekidis S, Schnitt SJ, Silver B, *et al.* The significance of extracapsular extension of axillary lymph node metastases in early-stage breast cancer. *Int J Radiat Oncol Biol Phys* 2000;46:31–34.
 29. Stranzl H, Mayer R, Ofner P, *et al.* Extracapsular extension in positive axillary lymph nodes in female breast cancer patients. Patterns of failure and indications for postoperative locoregional irradiation. *Strahlenther Onkol* 2004;180:31–37.
 30. Rytto N, Holm NV, Qvist N, *et al.* Influence of adjuvant irradiation on the development of late arm lymphedema and impaired shoulder mobility after mastectomy for carcinoma of the breast. *Acta Oncol* 1988;27:667–670.